



Cite this: *RSC Adv.*, 2017, 7, 32982

# Influence of different aid-sintering additives on the green-emitting $\beta$ -SiAlON:Eu<sup>2+</sup> phosphors

Hailong Wang,<sup>ID</sup> Zhiping Yang,<sup>\*</sup> Zhijun Wang,<sup>ID</sup> Xiuqin Dong, Dong Wei, Zhenling Li and Miaomiao Tian

In this study, the influences of different aid-sintering additives on the synthesis of  $\beta$ -SiAlON:Eu<sup>2+</sup> phosphor were investigated. The aid-sintering additives include oxides, fluorides, chlorides, and carbonates. The  $\beta$ -SiAlON:Eu<sup>2+</sup> phosphor, synthesized using different additives, was investigated in detail *via* spectroscopic data, X-ray diffraction, quantum efficiency, and scanning electron microscopy; the particle morphology and spectroscopic properties improved with the addition of different additives. Different additives have different influences on the morphology of  $\beta$ -SiAlON:Eu<sup>2+</sup>. Most oxide additives increase the diameter of  $\beta$ -SiAlON:Eu<sup>2+</sup>. Most fluoride additives increase the length of  $\beta$ -SiAlON:Eu<sup>2+</sup>. Particles with different morphologies can be obtained by adjusting the quantities of the oxide and fluoride additives. When combined with red phosphors,  $\beta$ -SiAlON:Eu<sup>2+</sup> will produce wider color gamut backlights than the traditional yttrium aluminum garnet.

Received 3rd May 2017  
 Accepted 13th June 2017

DOI: 10.1039/c7ra04961g

[rsc.li/rsc-advances](http://rsc.li/rsc-advances)

## 1. Introduction

White light-emitting diode (LED) is called the next generation of solid-state lighting. Especially, GaN-based LED is now a new and developing backlight technology for wide color gamut and high efficiency liquid crystal displays. Backlight materials need phosphors with high stability, luminous efficiency, and wide color gamut. Therefore, instead of YAG:Ce<sup>3+</sup>, green-emitting  $\beta$ -SiAlON:Eu<sup>2+</sup> and red-emitting CaAlSiN<sub>3</sub>:Eu<sup>2+</sup> for wide color gamut white LEDs have become a trend.<sup>1</sup> New  $\beta$ -SiAlON:Eu<sup>2+</sup> phosphor-based green oxynitride phosphors with the formula Si<sub>6-z</sub>Al<sub>2</sub>O<sub>2</sub>N<sub>8-z</sub> (z stands for the number of Si-N pairs substituted by Al-O pairs, 0 < z < 4.2)<sup>2,3</sup> have been created.

$\beta$ -SiAlON:Eu<sup>2+</sup> has excellent luminescence properties and high stability, which can be used for backlight displays as a green phosphor. However, generally, if no additives are added,  $\beta$ -SiAlON:Eu<sup>2+</sup> is not easy to be sintered, the fluorescent powder is small, the brightness is low, and the crystallinity is poor. Therefore, it is urgent to find a new method to improve the performance of  $\beta$ -SiAlON:Eu<sup>2+</sup>. As is known, a good additive can reduce the reaction temperature and reaction time and increase the reaction activity between molecules, which will be beneficial for the synthesis of  $\beta$ -SiAlON:Eu<sup>2+</sup> phosphors. However, currently, there are only a few studies on the synthesis of  $\beta$ -SiAlON:Eu<sup>2+</sup> phosphors using different additives.

In this study, the influence of different kinds of aid-sintering additives on the synthesis of  $\beta$ -SiAlON:Eu<sup>2+</sup> phosphor was

investigated. The aid-sintering additives include oxides, fluorides, chlorides, and carbonates. The properties of  $\beta$ -SiAlON:Eu<sup>2+</sup> phosphor synthesized using different additives were investigated *via* spectroscopic data, X-ray diffraction (XRD), quantum efficiency (QE), and scanning electron microscopy (SEM). Moreover, the factors that affect the formation of elongated  $\beta$ -SiAlON grains have been discussed.

## 2. Experimental

### 2.1. Materials and preparation

Samples of  $\beta$ -SiAlON:Eu<sup>2+</sup> were prepared in a glove box (N<sub>2</sub> < 0.1 ppm, H<sub>2</sub>O < 0.1 ppm) under a continuous flow of purified nitrogen. The starting materials Si<sub>3</sub>N<sub>4</sub> (UBE-10, containing 1.6% oxygen), AlN (Tokuyama Chemical Co., Ltd., E-grade), and Eu<sub>2</sub>O<sub>3</sub> (Aladdin, purity 99.99%) were stoichiometrically mixed in the composition: Eu<sub>0.043</sub>Si<sub>6.000</sub>Al<sub>0.194</sub>O<sub>0.064</sub>N<sub>8.221</sub>, with different aid-sintering additives, including oxides, fluorides, chlorides, and carbonates, and the weight of the aid-sintering additives is 1% of the total weight. Oxide additives include B<sub>2</sub>O<sub>3</sub> (Liaoning Banda Technology Co., Ltd, purity 98.8%), Bi<sub>2</sub>O<sub>3</sub> (Shanghai Cheng Xin Industrial Co., Ltd., purity 99.99%), Li<sub>2</sub>O (Ganzhou Keoming sharp non-ferrous metal materials Co., Ltd., purity 99%), TiO<sub>2</sub> (Shanghai Yuejiang Titanium Dioxide Chemical Products Co., Ltd., purity  $\geq$  92%), 5  $\mu$ m SiO<sub>2</sub> (Zhejiang Tongda Weipeng Electric Co., Ltd., purity 99.5%), BaO (Guangzhou Su Well Chemical Co., Ltd., purity  $\geq$  99.5%), Al<sub>2</sub>O<sub>3</sub> (Hangzhou Jikang New Material Co., Ltd., purity 99.999%), and Y<sub>2</sub>O<sub>3</sub> (Ganzhou Wanzhen Mineral Products Co., Ltd., purity 99%). Fluoride additives include NaF (Wengjiang chemical reagents source manufacturers, purity 98%), KF (Shanghai Ebi

College of Physics Science & Technology, Hebei Key Lab of Optic-Electronic Information and Materials, Hebei University, Baoding 071002, China. E-mail: yzp@ledphor.com; wangzj1998@126.com



Chemical Reagent Co., Ltd., purity 99%),  $\text{AlF}_3$  (Aladdin),  $\text{MgF}_2$  (Beijing Shengbo Gaotai Optical Technology Co., Ltd., purity 99.99%),  $\text{BaF}_2$  (Aladdin, purity 99%),  $\text{CaF}_2$  (Shanghai Rui Yu Photoelectric Material Co., Ltd., purity 99.9%), and  $\text{CeF}_3$  (Dongguan City Kayman Optoelectronics Technology Co., Ltd., purity 99.99%). Chloride additives include  $\text{SrCl}_2$  (Chongqing Qinglong fine strontium salt Chemical Co., Ltd., purity 99%),  $\text{KCl}$  (Shijiazhuang modern instrumentation Chemical Co., Ltd., purity 99%),  $\text{NaCl}$  (Tianjin Zhiyuan Chemical Reagent Co., Ltd., purity 99.5%),  $\text{MgCl}_2$  (Fuchen brand franchise stores, purity 98%),  $\text{CaCl}_2$  (Dongguan City Changan Jinghua of the operation of the instrument, purity 96%), and  $\text{LiCl}$  (Hefei Jiankun Chemical Co., Ltd., purity 97%). Carbonate additives include  $\text{Li}_2\text{CO}_3$  (Luoyang special resistant lining limited liability company, purity 99.9%),  $\text{BaCO}_3$  (Dongguan City Dongcheng Wantong Trade, purity 99%), and  $\text{Na}_2\text{CO}_3$  (Shijiazhuang Youjia Trading Company, purity 99.8%).

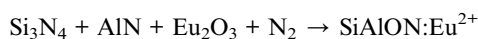
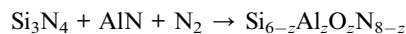
These starting materials were milled for about 60 minutes in a corundum mortar after lapping, and then, the mixture materials were placed in tungsten crucibles.

## 2.2 Process conditions

The material powder mixture was fired in a high gas-pressure sintering furnace. A high temperature and high pressure sintering furnace can be heated from 0 °C to nearly above 2200 °C, and the pressure ranging from 0 MPa to near 10 MPa was applied. The powder mixture was fired for 8 h at 2000 °C under a 2 MPa  $\text{N}_2$  atmosphere. The heating speed was 10 °C  $\text{min}^{-1}$  from room temperature to 1500 °C during the first sintering procedure. The temperature was increased to 2000 °C at the heating speed of 8 °C  $\text{min}^{-1}$  in the second sintering procedure. The powder mixture was synthesized by GPS at 2000 °C for 8 h under 2 MPa of  $\text{N}_2$  atmosphere. Then, it was finally cooled down to room temperature at 15 °C  $\text{min}^{-1}$ .

$\text{Eu}^{3+}$  ion in the starting powder  $\text{Eu}_2\text{O}_3$  was reduced to  $\text{Eu}^{2+}$  under a  $\text{N}_2$  atmosphere, which was confirmed by the absorption and emission spectra presented hereinafter.<sup>4</sup> As is known,  $\text{Eu}^{2+}$  has a broad emission and excitation band with high efficiency due to the allowed  $4f \rightarrow 5d$  electronic transitions.<sup>5</sup> The emission wavelength of  $\text{Eu}^{2+}$  in different hosts has alterable emission peaks, depending on the crystal field splitting occurring due to the surrounding ligands.

The general reaction for the synthesis of  $\beta$ -SiAlON phosphor powders is as follows:



## 2.3 Materials characterization

$\beta$ -SiAlON belongs to a hexagonal crystal system with a  $P6_3$  space group. To analyze the phase products of the as-prepared samples of the  $\beta$ -SiAlON: $\text{Eu}^{2+}$  powders, X-ray powder diffraction (XRD) was conducted using a D8A25 X-ray diffractometer from 10° to 80°

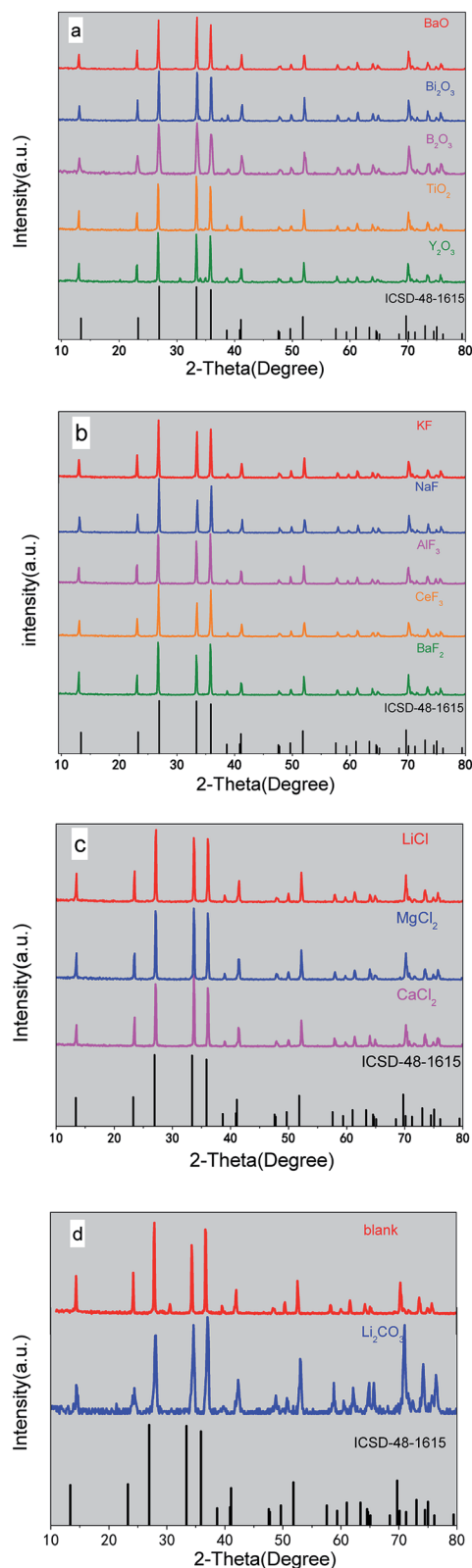


Fig. 1 (a) X-ray diffraction patterns of  $\text{Eu}^{2+}$ -doped  $\beta$ -SiAlON prepared with different oxide aid-sintering additives. (b) X-ray diffraction pattern of  $\text{Eu}^{2+}$ -doped  $\beta$ -SiAlON prepared with different fluoride aid-sintering additives. (c) X-ray diffraction pattern of  $\text{Eu}^{2+}$ -doped  $\beta$ -SiAlON with different chloride aid-sintering additives. (d) X-ray diffraction pattern of  $\text{Eu}^{2+}$ -doped  $\beta$ -SiAlON prepared with different carbonate aid-sintering additives.



with CuK $\alpha$  radiation ( $\lambda = 1.5418 \text{ \AA}$ ), operating at 40 kV and 40 mA and using the step size of  $0.02^\circ$  with a scan speed of  $0.5^\circ \text{ min}^{-1}$ .

Spectroscopic data was obtained using the high accuracy array spectral radiometer of HAAS-2000. The data measured by this device include luminance ( $L$ ), (Commission International de l'Eclairage (CIE), 1976)<sup>6</sup> X color chromaticity ( $X$ ), Y color chromaticity ( $Y$ ), emission peak (EM), and full widths at half maximum (FWHM).

Photoluminescence spectra of the  $\beta$ -SiAlON:Eu<sup>2+</sup> samples were obtained using a HORIBA FL-4600 fluorescence spectrophotometer with a Xe lamp as the excitation source. The scanning speed was 480 nm per minute, and the scanning wavelength ranged from 200 nm to 750 nm. The excitation spectra were checked for the spectral distribution of the Xe lamp intensity by measuring the photoluminescence spectrum for rhodamine-B.

Quantum efficiency (QE) was tested by Hitachi F-7000 with a Xe lamp as the excitation source. QE was measured by the excitation monochromator in the 280–480 nm range. A white Spectralon standard was illuminated with a resulting monochromatic light. The reflected light was collected using an integrating sphere and directed to a F-7000 multichannel photodetector; the spectrum was used for calibration. After this, the standard sample was replaced by the tested sample.<sup>7</sup>

Scanning electron microscopy (SEM) images were obtained using a Hitachi S-4800 field emission scanning electron microscope. The Hitachi S-4800 field emission scanning electron microscope features a maximum resolution of 1.0 nm and a variable acceleration voltage ranging from 5 kV to 30 kV.<sup>8</sup> The fluorescent images of  $\beta$ -SiAlON were obtained by a Canon 600D camera in a dark environment.

### 3. Results and discussions

#### 3.1 Phase identification

Fig. 1 shows the XRD patterns of  $\beta$ -SiAlON:Eu<sup>2+</sup> with different aid-sintering additives including oxides, fluorides, chlorides, and carbonates. The phase identification of  $\beta$ -SiAlON is provided in the JCPDS card no. 48-1615. It can be concluded that Eu<sup>2+</sup> has a relatively high solubility in the  $\beta$ -SiAlON host lattice.

#### 3.2 Photoluminescence properties

##### Spectroscopic data Part 1

Influence of different aid-sintering additives on the green-emitting  $\beta$ -SiAlON:Eu<sup>2+</sup> powder (Part 1)

|        | Additives and content (wt%)    | $L$   | $X$  | $Y$    | EM (nm) | FWHM (nm) |      |
|--------|--------------------------------|-------|--|--------|---------|-----------|------|
| Part 1 | Blank                          | 0     | 20.1   | 0.3012 | 0.6468  | 530.1     | 52.6 |
| oxide  | B <sub>2</sub> O <sub>3</sub>  | 1.00% | 16.6   | 0.3232 | 0.6342  | 538.3     | 55.9 |
|        | Bi <sub>2</sub> O <sub>3</sub> | 1.00% | 34.7   | 0.3238 | 0.6357  | 539.1     | 54.9 |
|        | Li <sub>2</sub> O              | 1.00% | The color of fracture surfaces was dark yellow |        |         |           |      |
|        | TiO <sub>2</sub>               | 1.00% | The color of fracture surfaces was black       |        |         |           |      |
|        | 5 $\mu\text{m}$                | 1.00% | 33.4   | 0.3183 | 0.6437  | 538       | 52.8 |
|        | SiO <sub>2</sub>               |       |  |        |         |           |      |

(Contd.)

Influence of different aid-sintering additives on the green-emitting  $\beta$ -SiAlON:Eu<sup>2+</sup> powder (Part 1)

|  | Additives and content (wt%)    | $L$   | $X$  | $Y$    | EM (nm) | FWHM (nm) |      |
|--|--------------------------------|-------|------|--------|---------|-----------|------|
|  | BaO                            | 1.00% | 18.7 | 0.3125 | 0.6393  | 536.4     | 55.3 |
|  | Al <sub>2</sub> O <sub>3</sub> | 1.00% | 29.9 | 0.3187 | 0.6427  | 538.3     | 53.3 |
|  | Y <sub>2</sub> O <sub>3</sub>  | 1.00% | 19   | 0.386  | 0.5807  | 537.9     | 73.5 |

The typical XRD patterns of  $\beta$ -SiAlON prepared with different aid-sintering additives are shown in Fig. 1. All the diffraction peaks could be indexed to the pure hexagonal-structured phase (JCPDS card no. 48-1615). Fig. 1(a)–(c) show the XRD pattern of the synthesized samples; the products of  $\beta$ -SiAlON are formed as a single-phased structure without secondary phases. The particles have high crystallinity because of the well-defined sharp diffraction peaks. However, from Fig. 2(d), we can see that there are no well-defined sharp diffraction peaks in the range from  $15^\circ$  to  $75^\circ$  for the Li<sub>2</sub>CO<sub>3</sub> additive. The small divergence between nominal and actual compositions of  $\beta$ -SiAlON may be ascribed to the existence of oxide impurities on the surfaces of raw and processed materials and formation of a small amount of amorphous phases on the surfaces of the crystallites. It is believed that the actual compositions of  $\beta$ -SiAlON are determined by the nominal compositions, and carbonate as an additive will influence the compositions of  $\beta$ -SiAlON. It can be seen from the XRD pattern that these additives have no effect on the main lattice structure of the  $\beta$ -SiAlON phosphor.

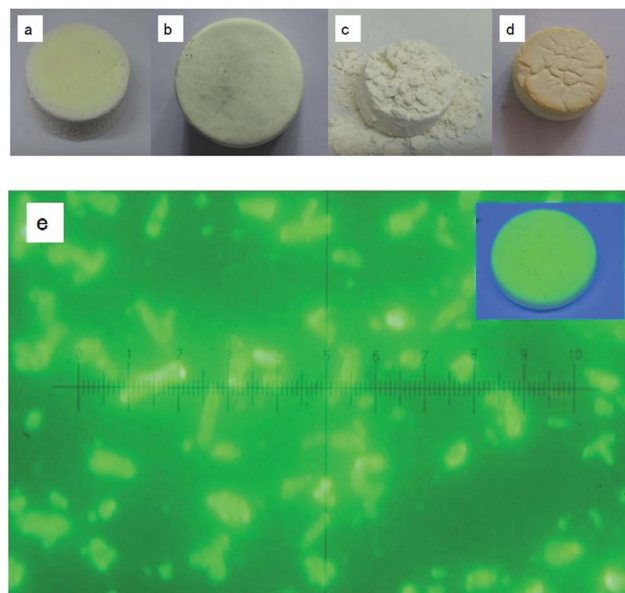


Fig. 2 The sectional images of  $\beta$ -SiAlON:Eu<sup>2+</sup> sintered materials with BaO (a), NaF (b), LiCl (c), and BaCO<sub>3</sub> (d). Blue light observed under the microscope with BaO (e).



## Spectroscopic data Part 2

Influence of different aid-sintering additives on the green-emitting  $\beta$ -SiAlON:Eu<sup>2+</sup> powder (Part 2)

| Additives and content (wt%) |                        | L  | X      | Y      | EM (nm) | FWHM (nm) |
|-----------------------------|------------------------|--|--------|--------|---------|-----------|
| Part 2 fluoride             | NaF 1.00%              | 21.9   | 0.3021 | 0.6505 | 537.1   | 52.4      |
|                             | KF 1.00%               | 17.1   | 0.2897 | 0.6491 | 529.4   | 51.5      |
|                             | AlF <sub>3</sub> 1.00% | 22.8   | 0.3238 | 0.635  | 538.7   | 54.8      |
|                             | MgF <sub>2</sub> 1.00% | The color of fracture surfaces was yellow and light green, low brightness        |        |        |         |           |
|                             | BaF <sub>2</sub> 1.00% | 27.2   | 0.306  | 0.6487 | 537.9   | 52.4      |
|                             | CaF <sub>2</sub> 1.00% | The color of fracture surfaces was dark yellow, additives may need to be reduced |        |        |         |           |
| CeF <sub>3</sub> 1.00%      | 18.2                   | 0.2899   | 0.6545 | 530.9  | 51.2    |           |

## Spectroscopic data Part 3

Influence of different aid-sintering additives on the green-emitting  $\beta$ -SiAlON:Eu<sup>2+</sup> powder (Part 3)

| Additives and content (wt%) |                         | L  | X      | Y      | EM (nm) | FWHM (nm) |
|-----------------------------|-------------------------|--|--------|--------|---------|-----------|
| Part 3 chloride             | SrCl <sub>2</sub> 1.00% | 24.2   | 0.3137 | 0.6447 | 537.2   | 53.4      |
|                             | KCl 1.00%               | 15.7   | 0.3312 | 0.6261 | 537.9   | 57.9      |
|                             | NaCl 1.00%              | 19.5   | 0.3152 | 0.6435 | 537.9   | 54.1      |
|                             | MgCl <sub>2</sub> 1.00% | The color of fracture surfaces was almost non-bright |        |        |         |           |
|                             | CaCl <sub>2</sub> 1.00% | The color of fracture surfaces was low bright        |        |        |         |           |
| LiCl 1.00%                  | 16.7                    | 0.3006   | 0.6445 | 531.3  | 53.9    |           |

## Spectroscopic data Part 4

Influence of different aid-sintering additives on the green-emitting  $\beta$ -SiAlON:Eu<sup>2+</sup> powder (Part 4)

| Additives and content (wt%) |                                 | L  | X  | Y | EM (nm) | FWHM (nm) |
|-----------------------------|---------------------------------|----|--|---|---------|-----------|
| Part 4 carbonate            | Li <sub>2</sub> CO <sub>3</sub> | 1% | The color of fracture surfaces was almost non-bright, and they had hard texture      |   |         |           |
|                             | BaCO <sub>3</sub>               | 1% | The color of fracture surfaces was almost non-bright, and they had very hard texture |   |         |           |
|                             | Na <sub>2</sub> CO <sub>3</sub> | 1% | The color of fracture surfaces was almost non-bright, and they had hard texture      |   |         |           |

The spectroscopic data were obtained *via* HAAS-2000. The quantity of every additive is 1% of the mass ratio, and the type of additives can be found in the table. From the spectroscopic data Part 1, we can see that most oxide additives will increase X. Moreover, from the spectroscopic data Part 2, we see that most fluoride additives used herein have a narrow FWHM from 51 to 52 nm. As is known,  $\beta$ -SiAlON has high-temperature mechanical properties.<sup>9</sup> During sintering, chloride additives can make  $\beta$ -

SiAlON sinter into a soft material. However, as presented in the spectroscopic data Part 3, the samples with chloride additives have low luminance. The carbonate additives investigated herein will cause  $\beta$ -SiAlON powders to severely contract. Carbonate additives are not appropriate for sintering  $\beta$ -SiAlON:Eu<sup>2+</sup>. Compared with the corresponding oxide, the carbonate has the extra substance which is carbon dioxide. From the spectroscopic data Part 2, we found that  $\beta$ -SiAlON:Eu<sup>2+</sup> with carbonate additives basically had no luminance. The morphology of the  $\beta$ -SiAlON particle with different additives can be observed using a scanning electron microscope (SEM).

Fig. 2 shows the sectional images of the  $\beta$ -SiAlON:Eu<sup>2+</sup> sintered materials from Fig. 2(a)–(d). Fig. 2(e) is imaged by L3201LED4 in B (the excitation wavelength is 450–470 nm) mode.

As shown in Fig. 2,  $\beta$ -SiAlON has the typical high hardness values, which is difficult to be processed in industry. It can be observed that the surface of the powder samples shown in Fig. 2(a) and (b) is smoother than that shown in Fig. 2(c). For phosphor powder, the more smooth the material, the harder it is to process. From Fig. 2(d), we can see the cracking phenomenon on the material surface, and the sample is the hardest to process. In Fig. 2(e), it is 400 times magnification under the blue light excitation (450–470 nm) with oxide additive BaO. The upper right corner of the picture is excited under the 365 nm light.

The photoluminescence (PL) spectra of the  $\beta$ -SiAlON:Eu<sup>2+</sup> powder with different aid-sintering additives are shown in Fig. 3. The excitation of the  $\beta$ -SiAlON:Eu<sup>2+</sup> is a direct process.<sup>10</sup> The excitation spectrum ranged from UV (350–410 nm) to visible light. The emission spectrum consists of a broadband from about 500 to 600 nm with a maximum at 535 nm, and the FWHM is less than 55 nm. Eu<sup>2+</sup> ions are lifted from the ground state of 4f<sup>7</sup> to the excited state of 4f<sup>6</sup>5d by forming e<sup>-</sup> valence electrons in the excited state and leaving h<sup>+</sup> holes in the ground state.

Fig. 3 illustrates the emission and excitation spectra of  $\beta$ -SiAlON:Eu<sup>2+</sup> particles with different additives. In the excitation spectra, under emission at 525 nm, there are two excitation bands centered from 290 nm to 420 nm, which are observed for the samples with different additives or no additive. The emission spectra show a single emission band peaked near 530 nm under the excitation at 285 nm, which should be due to the transition of Eu<sup>2+</sup> ions from 4f<sup>6</sup>5d to 4f<sup>7</sup>. PL intensities are different for different additives. There are promotional or inhibitory actions in the synthesis of  $\beta$ -SiAlON:Eu<sup>2+</sup> particles with different additives. Fig. 3(a) presents the emission and excitation spectra of  $\beta$ -SiAlON:Eu<sup>2+</sup> with and without BaO as an additive. It can be clearly seen that the emission intensity of the samples with BaO is much higher than those without it. The same phenomenon can be found in the samples with fluoride as an additive, as shown in Fig. 3(b). Fig. 3(c) presents the emission and excitation spectra of  $\beta$ -SiAlON:Eu<sup>2+</sup> particles with chloride as additives, and we can see that the intensity with chloride as additives is the lowest among those of all the other additives. Furthermore, the emission intensity of the samples, as shown in Fig. 3(d), with carbonate as additives is much lower



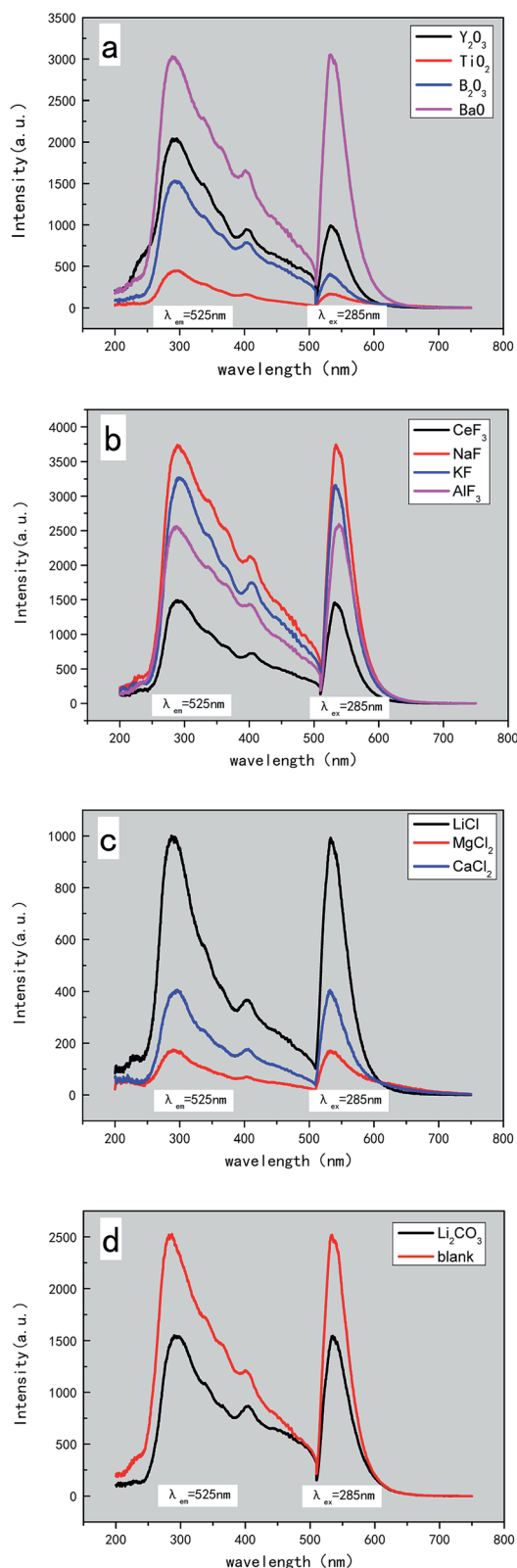


Fig. 3 Emission and excitation spectra of  $\beta$ -SiAlON:Eu<sup>2+</sup> ( $\lambda_{\text{ex}} = 285$  nm,  $\lambda_{\text{em}} = 525$  nm) with different kinds of additives.

than that of the samples with no additive. Therefore, although the addition of chloride additives make the material soft, it reduces the intensity of light emission and the degree of

crystallization; thus, the amount of chloride additives should be controlled. In addition, it is a wrong choice to use carbonates as additives for synthesizing  $\beta$ -SiAlON:Eu<sup>2+</sup>.

### 3.3 Quantum efficiency of the $\beta$ -SiAlON:Eu<sup>2+</sup>

$\beta$ -SiAlON:Eu<sup>2+</sup> phosphors can be efficiently excited over a wide spectral range from 280 to 480 nm. Moreover, it has an emission peak at 535 nm with a full width at half maximum (FWHM) less than 55 nm. It has superior color chromaticity of  $x = 0.32$  and  $y = 0.64$ . When the excitation wavelength is increased from 285 to 300 nm, the internal quantum efficiencies ( $\eta_i$ ) of  $\beta$ -SiAlON:Eu<sup>2+</sup> phosphor is more than 70%, and the external quantum efficiencies ( $\eta_o$ ) of  $\beta$ -SiAlON:Eu<sup>2+</sup> phosphor is more than 61%.<sup>11</sup> GaN chip-based LED is now an emerging back-light technology for wide color gamut and high efficiency liquid crystal displays.

External ( $\eta_o$ ) (1) and internal ( $\eta_i$ ) (2) quantum efficiencies (QEs) were calculated using the following equations:<sup>12</sup>

$$\eta_o = \frac{\int \lambda P(\lambda) d\lambda}{\int \lambda E(\lambda) d\lambda} \quad (1)$$

$$\eta_i = \frac{\int \lambda P(\lambda) d\lambda}{\int \lambda [E(\lambda) - R(\lambda)] d\lambda} \quad (2)$$

Fig. 4(a) shows the results of quantum yield calculation for the BaO additive. The internal quantum yield is 33.9%, the external quantum yield is 12.9%, the absorbance is 38.0%, the amount of absorption is 13 366.836, and the amount of fluorescence is 4532.686. Fig. 4(b) shows the results of the quantum yield calculation for the NaF additive. The internal quantum yield is 50.7%, the external quantum yield is 15.4%, the absorbance is 30.4%, the amount of absorption is 10 718.719, and the amount of fluorescence is 5432.117.

As is known, QE is affected by the probability of the non-radiative processes. The non-radiative recombination is reduced when the phosphors are well crystallized. The QE can be improved by controlling the particle size, size distribution, and morphology through the processing conditions. The morphology and the particle size can be influenced by doping different additives.

### 3.4 Morphology of the $\beta$ -SiAlON

Gold was used to coat all the experimental samples before the SEM observation. Fig. 5 shows the SEM images of the  $\beta$ -SiAlON:Eu<sup>2+</sup> powder phosphors with different aid-sintering additives. Nucleation and growth are the two steps of the  $\beta$ -SiAlON forming process. The powders consist of rod-like crystals with no additive, as shown in Fig. 5(e), which are 3–4  $\mu\text{m}$  in length and about 1–1.5  $\mu\text{m}$  in diameter. However, from the other 4 images, we can see different things. In Fig. 5(c) and (d), we found that the length of  $\beta$ -SiAlON:Eu<sup>2+</sup> is much longer than that of the sample shown in Fig. 5(e); the length is more than 10  $\mu\text{m}$  when fluoride additives are used. In Fig. 5(a) and (b), we found



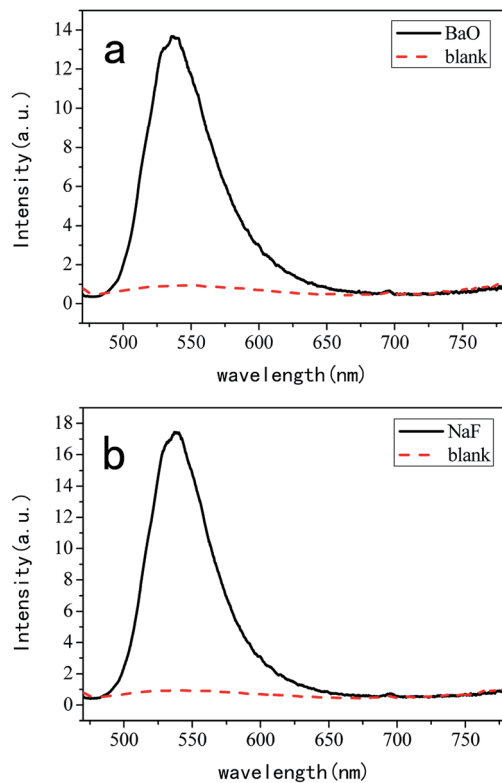


Fig. 4 Quantum yield of  $\beta$ -SiAlON:Eu<sup>2+</sup> with BaO (a) and NaF (b).

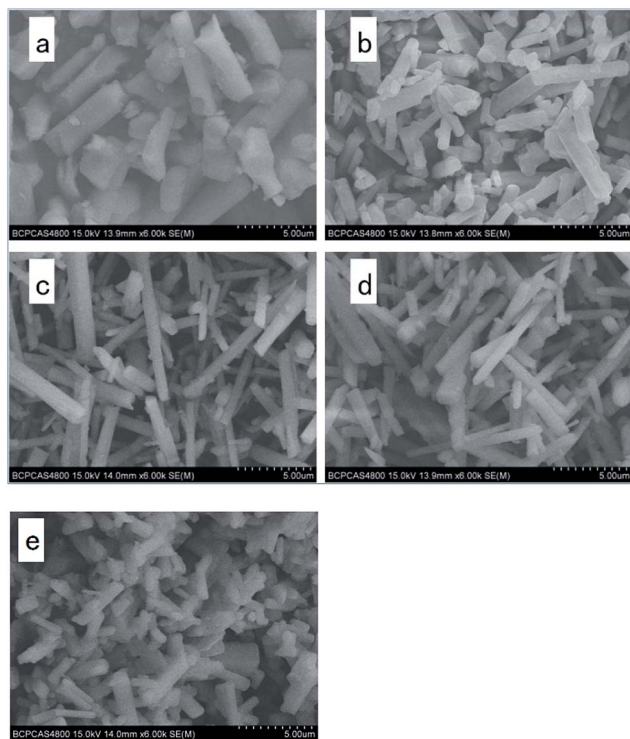


Fig. 5 SEM images of the morphology of  $\beta$ -SiAlON:Eu<sup>2+</sup> with Bi<sub>2</sub>O<sub>3</sub> (a), BaO (b), NaF (c), KF (d), and no additive (e).

that the diameter of  $\beta$ -SiAlON:Eu<sup>2+</sup> is more than that of the sample shown in Fig. 5(e). Thus, we can conclude that fluoride additives can result in a longer morphology, whereas oxide additives can result in a wider morphology.

## 4. Conclusions

The influences of different aid-sintering additives on the synthesis of  $\beta$ -SiAlON:Eu<sup>2+</sup> phosphor have been investigated.

The addition of good additives will increase the crystallinity of the particles, thus resulting in a much narrower FWHM. Most of the  $\beta$ -SiAlON:Eu<sup>2+</sup> samples prepared herein have a narrow FWHM of less than 55 nm.

Different additives influence the crystallinity of  $\beta$ -SiAlON:Eu<sup>2+</sup>. Some oxide and fluoride additives can make the crystallinity increase. However, carbonate additives have the opposite effect. Carbonate additives also increase the hardness, and it becomes hard to break the block into powders.

Different additives influence the spectroscopic data of  $\beta$ -SiAlON:Eu<sup>2+</sup>. Most oxide additives increase the brightness of  $\beta$ -SiAlON:Eu<sup>2+</sup>. Most fluoride additives will cause  $\beta$ -SiAlON:Eu<sup>2+</sup> to have a narrow FWHM from 51 nm to 52 nm. These two kinds of additives may enhance the crystallinity of the particles. Carbon dioxide is a bad influencing factor in the synthesis of  $\beta$ -SiAlON:Eu<sup>2+</sup> powders. Therefore, it is significant to maintain a stable pressure and guarantee a good seal of the sintering furnace during the process of sintering. Before heating the sintering furnace, it should be ensured that there is almost no carbon dioxide except for N<sub>2</sub>. Therefore, to obtain  $\beta$ -SiAlON:Eu<sup>2+</sup> powders with a larger particle size and a higher brightness, oxide additives should be added; if the FWHM needs to be narrowed, the appropriate fluoride additives should be added; moreover, if soft material is needed, chloride additives should be added.

## Acknowledgements

One of the authors is grateful to Hebei Ledphor Optoelectronics Technology Co. Ltd for the high temperature and high pressure sintering furnace, the College of Physical Science and Technology of Hebei University for XRD analysis, and the Beijing Physical and Chemical Test Center for the SEM analysis.

## Notes and references

- 1 R. J. Xie, N. Hirotsuki and T. Takeda, Wide color gamut backlight for liquid crystal displays using three-band phosphor-converted white light-emitting diodes, *Appl. Phys. Express*, 2009, 2(2), 022401.
- 2 Y. Oyama and O. Kamigaito, Solid solubility of some oxides in Si<sub>3</sub>N<sub>4</sub>, *Jpn. J. Appl. Phys.*, 1971, 10, 1347–4065.
- 3 K. H. Jack and W. I. Wilson, Ceramics based on the Si–Al–ON and related systems, *Nature*, 1972, 238, 0028–0836.
- 4 R.-J. Xie, N. Hirotsuki, M. Mitomo, Y. Yamamoto, T. Suehiro and K. Sakuma, Optical properties of Eu<sup>2+</sup> in  $\alpha$ -SiAlON, *J. Phys. Chem. B*, 2004, 108, 1520–6106.



- 5 D. Jia, R. S. Meltzer, W. M. Yen, W. Jia and X. Wang, Green phosphorescence of  $\text{CaAl}_2\text{O}_4: \text{Tb}^{3+}, \text{Ce}^{3+}$  through persistence energy transfer, *Appl. Phys. Lett.*, 2002, **80**, 0003–6951.
- 6 Y. Fukuda, N. Matsuda, A. Okada and I. Mitsuishi, White light-emitting diodes for wide-color-gamut backlight using green-emitting Sr-Sialon phosphor, *Jpn. J. Appl. Phys.*, 2012, **51**, 1347–4065.
- 7 L. Liu, R. J. Xie, N. Hirotsuki, *et al.*, Photoluminescence properties of  $\beta\text{-SiAlON: Yb}^{2+}$ , a novel green-emitting phosphor for white light-emitting diodes, *Sci. Technol. Adv. Mater.*, 2011, **12**(3), 034404.
- 8 G. R. Chalmers, R. M. Bustin and I. M. Power, Characterization of gas shale pore systems by porosimetry, pycnometry, surface area, and field emission scanning electron microscopy/transmission electron microscopy image analyses: examples from the Barnett, Woodford, Haynesville, Marcellus, and Doig units, *AAPG Bull.*, 2012, **96**, 0149–1423.
- 9 M. H. Bocanegra-Bernal and B. Matovic, Mechanical properties of silicon nitride-based ceramics and its use in structural applications at high temperatures, *Mater. Sci. Eng., A*, 2010, **527**, 0921–5093.
- 10 R. J. Xie, N. Hirotsuki, H. L. Li, Y. Q. Li and M. Mitomo, Synthesis and Photoluminescence Properties of  $\beta\text{-sialon: Eu}^{2+}(\text{Si}_{6-z}\text{Al}_z\text{O}_z\text{N}_{8-z}: \text{Eu}^{2+})$  A Promising Green Oxynitride Phosphor for White Light-Emitting Diodes, *J. Electrochem. Soc.*, 2007, **154**, 0013–4651.
- 11 N. Hirotsuki, R.-J. Xie, K. Kimoto, T. Sekiguchi, Y. Yamamoto, T. Suehiro and M. Mitomo, Characterization and properties of green-emitting  $\beta\text{-SiAlON: Eu}^{2+}$  powder phosphors for white light-emitting diodes, *Appl. Phys. Lett.*, 2005, **86**, 0003–6951.
- 12 K. Ohkubo and T. Shigeta, Absolute fluorescent quantum efficiency of NBS phosphor standard samples, *J. Illum. Eng. Inst. Japan*, 1999, **83**, 87–93.

